Nuclear Physics A539 (1992) 75–96
North-Holland

NUCLEAR
PHYSICS A

Radiative capture of protons by light nuclei at low energies

F.E. Cecil, D. Ferg, H. Liu, J.C. Scorby and J.A. McNeil
Department of Physics, Colorado School of Mines, Golden, Colorado 80401, USA

P.D. Kunz
Nuclear Physics Laboratory, University of Colorado, Boulder, Colorado 80302, USA

Received 18 January 1991
(Revised 24 September 1991)

Abstract: Gamma-ray-to-charged-particle branching ratios, and gamma-ray angular distributions have been measured for the radiative capture of protons by ^{6}Li, ^{7}Li, ^{9}Be and ^{11}B for proton bombarding energies between 40 and 180 keV. Except for the 163 keV resonance in the reaction ^{11}B(p, γ)^{12}C, the branching ratios are roughly independent of energy and the angular distributions are isotropic. These measurements are used to deduce reaction S-factors and infer thermonuclear reactivities. The measurements are compared to distorted-wave-Born-approximation direct-capture cross-section calculations.

1. Introduction

As part of a continuing program of measurements of radiative capture reactions of light ions by low-Z nuclei at low energies, we have investigated the radiative capture of protons by ^{6}Li, ^{7}Li, ^{9}Be and ^{11}B. Our earlier measurements were devoted to the radiative capture of deuterons on ^{3}H [ref. [1])], ^{2}H [ref. [2])], and ^{3}He [ref. [3])]. The immediate justification for these earlier measurements lay in the application to the prompt gamma-ray diagnostics of the current generation of controlled fusion plasma devices. The present set of measurements will likewise provide the data base for the analogous diagnostics of the advanced fuel fusion reactors. In addition, some of these results should prove applicable to current models of primordial nucleosynthesis.

While there have been highly accurate, fairly recent measurements of the reactions ^{6}Li(p, ^{3}He)^{4}He [ref. [4])], ^{7}Li(p, α)^{4}He [ref. [5])], ^{9}Be(p, α)^{6}Li [ref. [6])] and ^{11}B(p, α)^{8}Be [ref. [7])], at laboratory bombarding energies down to 23, 28, 30 and 24 keV respectively, there has been, with one exception, no reported measurements of the cross sections for the radiative capture of protons on these targets at energies below about 200 keV. The single exception consists of the well studied resonance in the reaction ^{11}B(p, γ)^{12}C at a proton bombarding energy of 163 keV [ref. [8])].

2. Experimental procedures

Our study consisted of thick-target γ-ray-to-charged-particle branching ratio measurements. These branching ratios were determined by concurrent measurements of the γ-ray and charged-particle spectra during the bombardment of the appropriate targets by analyzed proton beams from the Colorado School of Mines low-energy charged-particle accelerator [9]). This experimental procedure had been followed in earlier studies [1-3,10]). Advantages of this procedure include being able to bombard the target with moderately large beam currents, an insensitivity to the precise chemical or isotopic nature of the targets, an insensitivity to beam-charge collection efficiency, an insensitivity to details of the target stopping power, and an insensitivity to an exact knowledge of the beam energy. The disadvantage is that the yield of both the γ-rays and charged particles necessarily represent integrals over incident energy as the protons slow down in the target rather than representing the yields at a well-determined energy. A list of the reactions which we investigated, including the energies of the charged reaction products as well as the γ-rays is given in table 1.

A schematic picture of the experimental set-up is presented in fig. 1. In this figure, the beam from the accelerator enters the scattering chamber from the left and the target is located in the center of the chamber. Beam currents typically were tens of microAmperes. Accumulated charges at the lower energies were hundreds of milli Coulombs. The particle detector consisted of a 300 mm^2 silicon surface barrier (SSB) detector located at 90° from the beam direction at a distance of 10 cm from the target. In fig. 1, the gamma detector is depicted with the front face at a distance of 20 cm, from the target and positioned at an angle of 0° from the beam direction. By locating the gamma detector farther from the target we were able to measure

TABLE 1

Reactions studied in present work. The energies of the reaction products are for zero energy incident protons

Initial state	Charged particle final state (MeV)	Radiative capture final state (MeV)	Gamma ray energies (MeV)
$p+{}^6Li$	$^3He\,(2.29)+{}^4He\,(1.72)$	$^7Be\,(0.0)$	5.606
		$^7Be\,(0.429)$	5.177
$p+{}^7Li$	$2\times{}^4He\,(8.67)$	$^8Be\,(0.0)$	17.254
		$^8Be\,(3.04)$	14.214 [a])
$p+{}^9Be$	$^4He\,(1.27)+{}^6Li\,(0.84)$	$^{10}B\,(0.0)$	6.587
		$^{10}B\,(0.718)$	5.869
		$^{10}B\,(1.740)$	4.847
		$^{10}B\,(2.154)$	4.443
$p+{}^{11}B$	$^4He\,(5.73)+{}^8Be\,(2.86)$	$^{12}C\,(0.0)$	15.956
		$^{12}C\,(4.439)$	11.517

[a]) The 3.04 MeV level in ^8Be has a natural width $\Gamma = 1.5$ MeV.

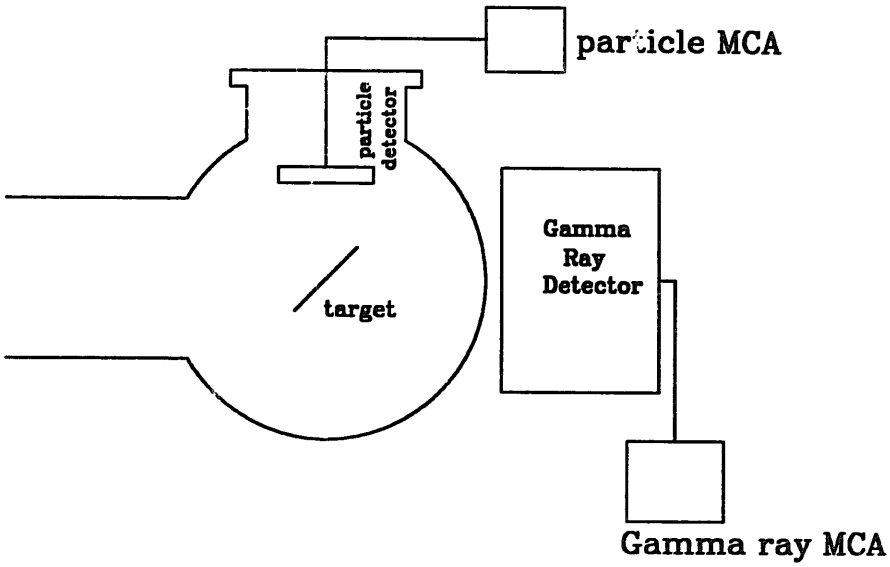

Fig. 1. Schematic layout of experimental set-up used in measurements of γ-ray-to-charged particle branching ratio.

angular distributions out to a maximum laboratory angle of 150° from the beam direction. The charged-particle detectors were assumed to have unit absolute detection efficiency. The energy calibration of the charged-particle detector was determined with a ^{241}Am source. The energy calibration of the γ-ray spectrometer was determined at low γ-ray energies with commercially obtained isotopic γ-ray sources, including the 4.44 MeV γ-ray from a PuBe source. At higher energies, the γ-ray energy calibration was accomplished using the 4.44, 11.67 and 16.11 MeV γ-rays from the reaction ^{11}B(p, γ)^{12}C at the 163 keV resonance [8]). The γ-ray spectra were measured using both a HARSHAW NaI(Tl) scintillation spectrometer with a Compton and cosmic-ray suppression shield and an ORTEC HpGe intrinsic germanium semiconductor spectrometer. The NaI(Tl) system, including a discussion of the absolute detection efficiency for γ-ray energies up to 16 MeV, has been published [11]). The HpGe detector was used to provide an independent measurement of the branching ratios when higher γ-ray energy resolution was needed. An in-situ measurement of the absolute full-energy and escape peaks detection efficiencies for the HpGe detector from 0.3 to 11.7 MeV was made at the lower energies using commercially obtained isotopic sources and at the higher energies with pairs of reaction γ-rays of different energies and known production ratios. This method of absolute detection efficiency determination has been described elsewhere [12]). In our determination, we used the 429 and 5306 keV γ-rays produced in the reaction ^{6}Li(p, γ)^{7}Be and the 4439 and 11670 keV γ-rays produced in the reaction ^{11}B(p, γ)^{12}C reaction to extend the efficiency from low to high energies. Both of these γ-ray pairs are produced with equal probability at the energies of our investigation. The absolute efficiencies thus determined are plotted in fig. 2. A quadratic fit through the measured data points is used to extrapolate the maximum energy of 11.7 MeV at which the

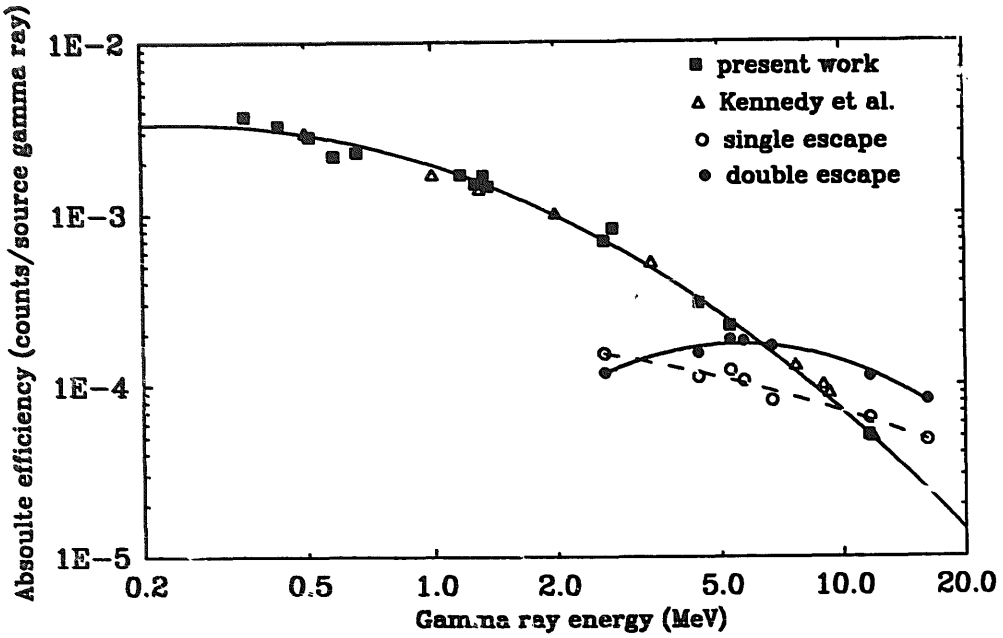

Fig. 2. Absolute detection efficiency of the HpGe γ-ray detector. The front face of the detector is located 8.0 cm from the center of the target. Our measurements of the full energy peak efficiencies (solid squares) are compared to the relative efficiencies at comparable energies reported by Kennedy *et al.* [13]). In addition we include our measurements of the absolute detection efficiencies of the first and second escape peak (solid and open circles). The first and second escape peak efficiencies at 16 MeV were determined relative to our extrapolation of the full energy peak efficiency.

efficiency is measured to 16 and 17 MeV as required for the ground-state transitions in ^{8}Be and ^{12}C. Our data are compared in fig. 2 to the relative detection efficiency determined at comparable energies by Kennedy *et al.* [13]).

Assuming isotropic production of both particles and γ-rays, the measured ratio of the yields $Y_\gamma(E_0)$ and $Y_p(E_0)$ of the γ-rays and charged particles may then be expressed:

$$\frac{Y_\gamma(E_0)}{Y_p(E_0)} = \left[\frac{\mathrm{eff}_\gamma(E_\gamma)}{\mathrm{eff}_p(E_p)}\right] \frac{\int [\sigma_\gamma(E) f(E)/\varepsilon(E)]\,\mathrm{d}E}{\int [\sigma_p(E) f(E)/\varepsilon(E)]\,\mathrm{d}E}, \tag{1}$$

where:

E_0 is the incident proton bombarding energy,

eff's are the respective detector efficiencies at the appropriate energies,

σ's are the total reaction cross sections at a center-of-mass energy E,

$f(E)$ is the atomic fraction of the target nucleus at a location in the target at which the incident beam energy has been reduced to E,

ε is the stopping power of the target for protons, again at a depth below the surface of the target where the incident beam energy has been reduced to E. We calculated the stopping powers using the code TRIM [14]).

The limits of integration are 0 and E_0.

If we define $BR(E_0)$ to be the ratio of the production rates of γ-rays to charged particles, then:

$$BR(E_0) = [Y_\gamma(E_0)/\mathrm{eff}_\gamma(E_\gamma)]/[Y_p(E_0)/\mathrm{eff}_p(E_p)]\,. \tag{2}$$

The reaction cross sections may be expressed in terms of the astrophysical S-factors:

$$\sigma(E) = (S(E)/E)\,\mathrm{e}^{-b/\sqrt{E}} \tag{3}$$

where the Gamow factor $b = 31.27 Z_T \mu^{1/2}(\mathrm{keV}^{1/2})$ with Z_T being the charge of the target, μ the proton-target reduced mass in a.m.u. and E the center-of mass energy in keV. Accordingly, the thick-target branching ratio is:

$$BR(E_0) = \frac{\int [S_\gamma(E)\,\mathrm{e}^{-b/\sqrt{E}} f(E)/(E\varepsilon(E))]\,\mathrm{d}E}{\int [S_p(E)\,\mathrm{e}^{-(b/\sqrt{E})} f(E)/(E\varepsilon(E))]\,\mathrm{d}E}\,. \tag{4}$$

The measured yield ratios as a function of proton bombarding energy E_0 and the previously determined [4-7]) S-factors $S_p(E)$ for the particle branches of the reactions then allow the S-factors $S_\gamma(E)$ for the γ-ray branches to be determined by assuming a value for the function $S_\gamma(E)$ which best reproduces the measured ratio $Y_\gamma(E)/Y_p(E)$. In practice, since the Coulomb penetration factor $e^{-(b/\sqrt{E})}$ in both integrands in eq. (4) decreases precipitously at low energies, the values of both integrals are equally proportional to the respective values of $S(E)$ at the upper limits on the integrals. A rough estimate of the γ-ray S-factor at a given bombarding energy E_0 is thus obtained:

$$\begin{aligned} S_\gamma(E_0) &\simeq S_p(E_0)[Y_\gamma(E_0)/Y_p(E_0)][\mathrm{eff}_p(E_p)/\mathrm{eff}_\gamma(E_\gamma)] \\ &\simeq S_p(E_0)BR(E_0)\,. \end{aligned} \tag{5}$$

As noted above, eqs. (1), (2), (4) and (5) assume spatial isotropy for both the charged particle and γ-ray branches of the capture reactions. Angular distributions have been measured for the energies under consideration in the case of the charged-particle branches [4-7]). Angular distributions of the γ-rays are measured in the present work and corrections arising from anisotropies in either particle or γ-ray angular distributions are applied where necessary.

3. Experimental results

In this section we present the results of our measurements of the branching ratios of the bombardment by protons of ^{6}Li, ^{7}Li, ^{9}Be and ^{11}B, the basic technique of which was described in the preceding section. The targets for the four measurements consisted, respectively, of rolled metallic Li foils, isotopically enriched to 94% in ^{6}Li, pressed powder pellets of natural LiF, commercially obtained thick foils of

metallic Be and pressed powder pellets of natural B. Charged-particle spectra measured during the bombardment of these targets are shown in fig. 3. The energies of the various particle groups are given in table 1. The energy calibrations for the ^{6}Li, ^{7}Li, ^{9}Be spectra are identical. From these spectra, the quantities $Y_p(E_0)$ were extracted and used in eq. (2) to determine the quantities BR(E_0). In the ^{6}Li spectra (fig. 3a), either the ^{3}He or the ^{4}He peak could be used to determine the quantity $Y_p(E_0)$. In the ^{7}Li spectra (fig. 3b), the outgoing charged particles are identical,

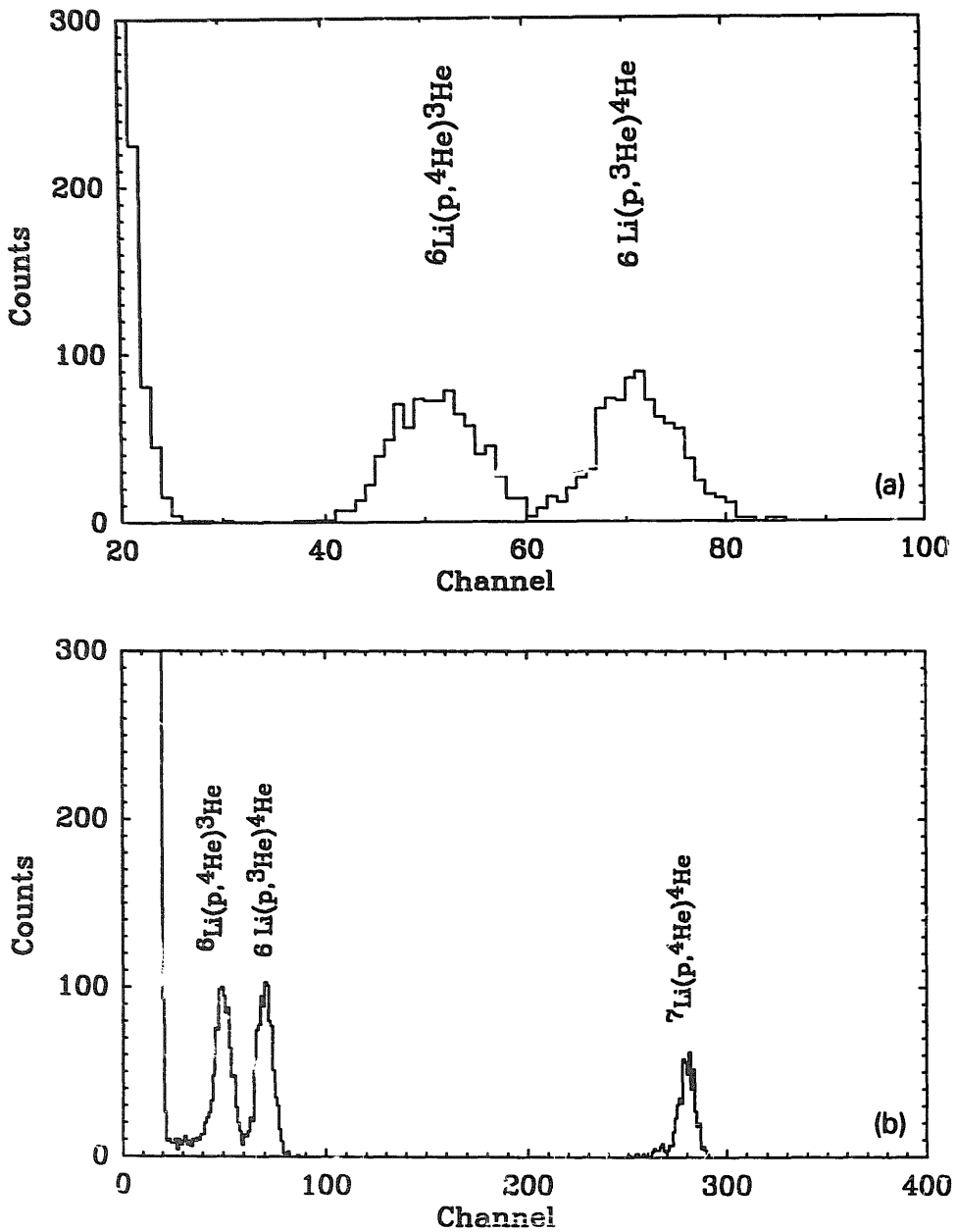

Fig. 3. Typical charged-particle spectra recorded during branching-ratio measurements. Parts (a)-(d) correspond respectively to the ^{6}Li, ^{7}Li, ^{9}Be and ^{11}B targets. The energies of the particles are identified in table 1. The bombarding energies at which the spectra in (a) and (b) were recorded was 150 keV. The bombarding energies for (c) and (d) were 140 and 165 keV, respectively.

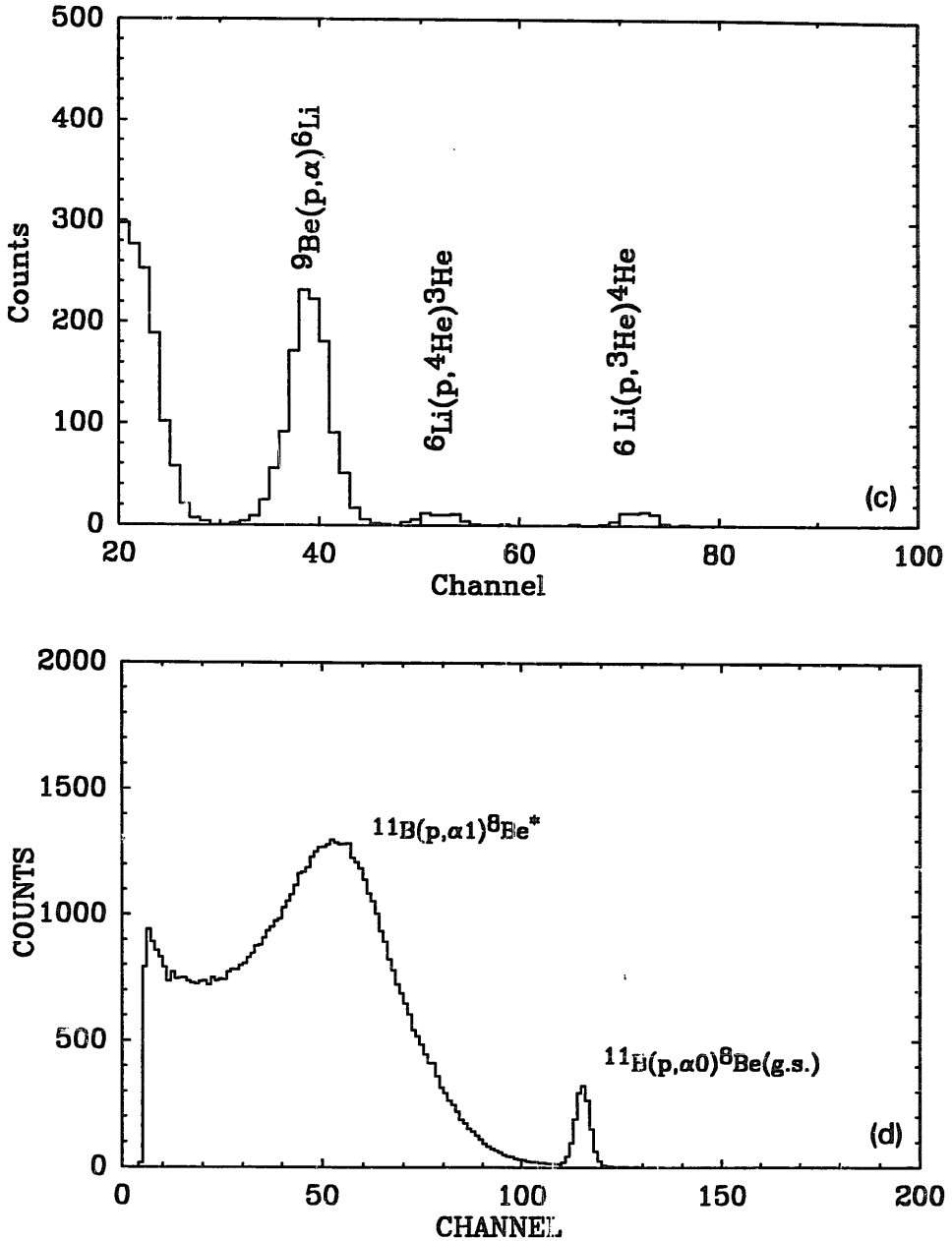

Fig. 3—continued.

each being an 8 MeV α-particle. Consequently the quantity $Y_p(E_0)$ was determined from one-half the number of counts in the peak labelled ^{7}Li(p, ^{4}He)^{4}He. In the ^{9}Be spectra, the outgoing ^{6}Li was not resolved from the low-energy detector noise and hence the quantity $Y_p(E_0)$ was, of necessity, derived from the number of counts in the peak labelled ^{9}Be(p, α)^{6}Li. In the ^{11}B spectrum, the broad group of α-particles corresponding to the transition to the ^{8}Be first excited state is only partially resolved from the low-energy continuum corresponding to the α-particle break-up of the residual ^{8}Be nuclei. Accordingly, the quantity $Y_p(E_0)$ is determined from the yield of the transition to the ^{8}Be ground state.

As noted above, eqs. (1) and (2) assume isotropic production of the charged particles. The angular distributions for the charged-particle reaction products from the ^{6}Li, ^{7}Li, and ^{9}Be reactions have been measured down to c.m. energies of 136,44, and 110 keV, respectively, and are nearly isotropic [4-6]). These energies overlap with the energies of the present study. The maximum measured anisotropy is about 4% in the case of the reaction ^{7}Li(p, ^{4}He)^{4}He at a c.m. energy of 136 keV. We assumed that the approximate isotropy in the angular distributions continued to lower energies. Consequently the quantities $Y_p(E_0)$ are related to the number of peak counts in the appropriate spectra by a simple geometric factor. In the case of the ^{11}B measurement, the angular distribution for the α-particle to the ^{8}Be ground state is not isotropic but is approximately asymmetric about 90° [ref. [7])]. Consequently, since the charged-particle detector is located at an angle of 90° with respect to the proton beam direction (see fig. 1), the quantity $Y_p(E_0)$ is likewise related to the number of counts in the α_0 peak (see fig. 3d) by a simple geometric factor. Therefore, in the case of ^{11}B, eqs. (1) and (2) are still appropriate even though the angular distribution is not isotropic.

The γ-ray spectra are shown in fig. 4 for the NaI(Tl) detector and for the HpGe detector in fig. 5. From these spectra, the quantities $Y_\gamma(E_0)$ were extracted and used in eq. (2) to determine the quantities BR(E_0). In the NaI(Tl) spectra, the anticoincidence shield suppresses the first escape peak by about a factor of two. The second escape peak is reduced by about a factor of ten. The extent to which the second escape peak is visible in the NaI(Tl) spectra was observed to depend on the energy of the γ-ray. This is seen in fig. 4d which shows the 16.11, 11.67 and 4.44 MeV γ-rays from the reaction ^{11}B(p, γ)^{12}C. The second escape peak from the 4.44 MeV γ-ray is clearly visible but not apparent in the case of the 11.67 or 16.11 MeV γ-rays. The second escape peaks in the case of the higher energy gamma rays are obscured in part since the absolute resolution of the individual peaks increases with increasing energy (hence the absolute width of the second escape peaks broadens). Other factors, such as more prominent edge effects arising from the greater ranges of the pair produced electrons and positrons, could likewise obscure the second escape peaks at higher energies. None the less, the peak regions of the individual γ-rays are well defined and it was not necessary to fit to a specific peak shape.

In the measurements on ^{7}Li and ^{11}B, the peak regions of γ-rays corresponding to capture to the ground and excited states could be resolved using the NaI(Tl) spectra. For these two nuclei the quantity BR(E) was measured for the individual nuclear states with the NaI(Tl) detector over the full energy range of the experiment and verified at the higher energies with the HpGe detector. For the measurements on ^{6}Li and ^{9}Be, however, the peak regions of the γ-rays corresponding to capture to the ground and excited states overlapped. For these two nuclei the total BR(E) was measured with the NaI(Tl) and the BR(E) to the individual nuclear states was measured only with the HpGe detector at the higher energies. The lowest energies at which the measurements were made were determined by the requirement of a

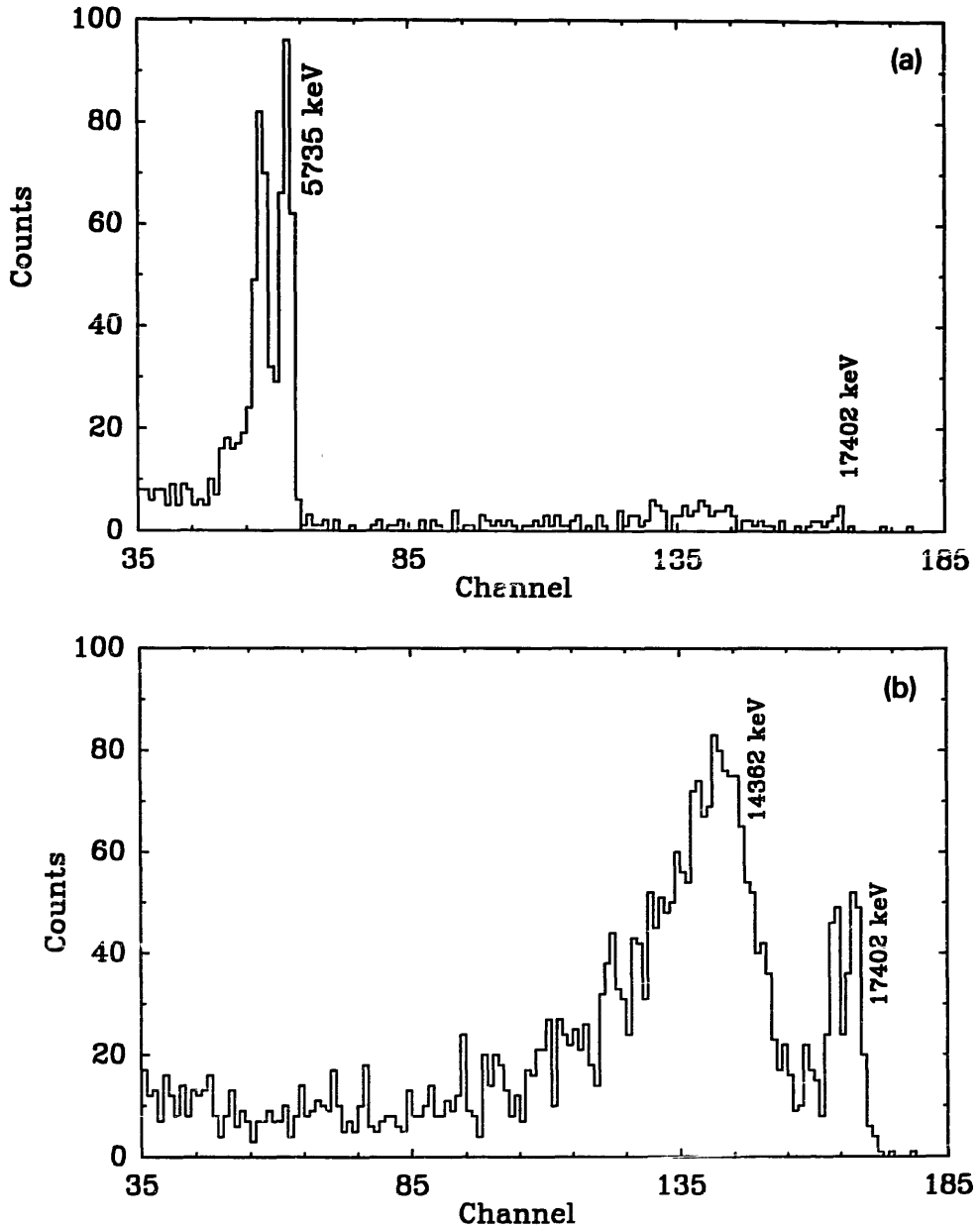

Fig. 4. Typical γ-ray spectra measured with the NaI(Tl) spectrometer system during the branching-ratio measurements. (a)-(d) correspond respectively to the ^{6}Li, ^{7}Li, ^{9}Be and ^{11}B targets. The transitions to which these γ-rays correspond are identified in table 2. The energies at which these spectra and those in fig. 5 were recorded are the same as indicated in fig. 3. All the gamma spectra in figs. 4 and 5 were recorded with the γ-ray detector positioned at 0° relative to the beam direction. The labels 1E and 2E refer to the single and double escape peaks. The 2.614 MeV background γ-ray from environmental Th is indicated in some of the spectra in figs. 4 and 5.

minimum statistical accuracy of about 20% in the yield of the γ-ray. Because of the small BR(E) values, the statistical accuracy in the measured yields of the charged particles was uniformly much greater than that of the γ-rays. This requirement imposed counting times typically of a day at the lowest energies. The only background which was encountered was that of a continuum in the spectra from cosmic-ray

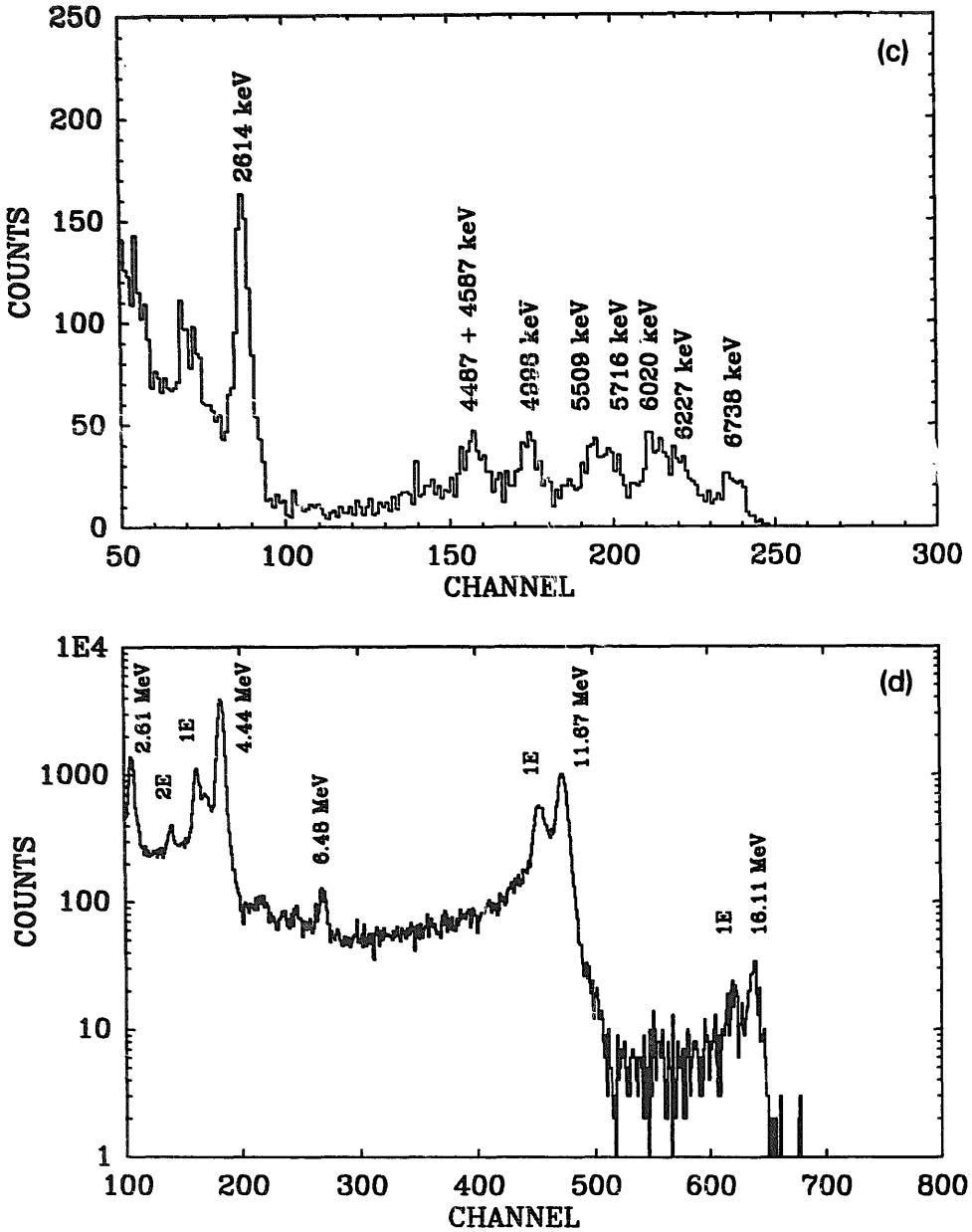

Fig. 4—continued.

signals which were not vetoed by the annular shield. This background is described in more detail in our earlier report on this detector system [11]). The highest energy discrete background γ-ray which was observed in the spectra was the 2.61 MeV line from the naturally occurring thorium in the environment. This line was lower in energy than the γ-rays from the capture reactions under investigation and hence did not constitute a significant interference.

The resulting BR(E) values for the four capture reactions are shown in fig. 6 as a function of center-of-mass energy. In the case of ^{6}Li, ^{7}Li, and ^{9}Be, the BR(E) values are nearly independent of energy. In the case of ^{11}B, however, the BR(E)

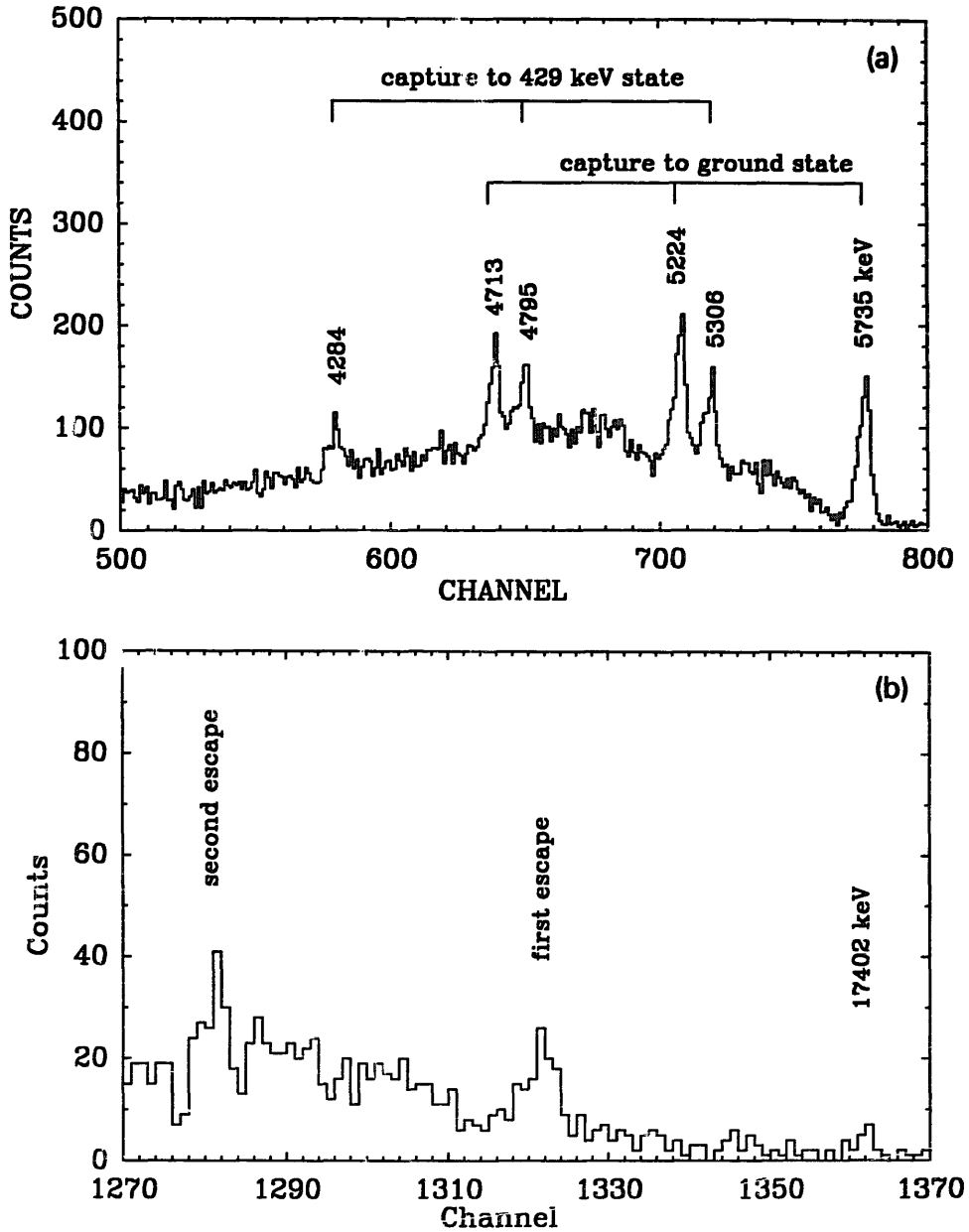

Fig. 5. Typical γ-ray spectra measured with the HpGe spectrometer during the branching ratio measurements. (a)-(d) correspond respectively to the ^{6}Li, ^{7}Li, ^{9}Be and ^{11}B targets. The transitions to which these γ-rays correspond are identified in table 2.

values change significantly at bombarding energies well below the peak of the 163 keV resonance. In fig. 6, the branching ratios for ^{6}Li and ^{9}Be represent the total γ-ray-to-charged-particle branching ratios, whereas in the cases of ^{7}Li and ^{11}B, the branching ratios to the ground and first excited states are plotted individually. As discussed above, these branching ratios may be used, together with eq. (4), to determine the S-factors for the γ-ray production reactions. The S-factors so determined are given in table 2, where we include the relative γ-ray branching ratios. The S-factors derived using eq. (4) agree within 10% with the estimates of the

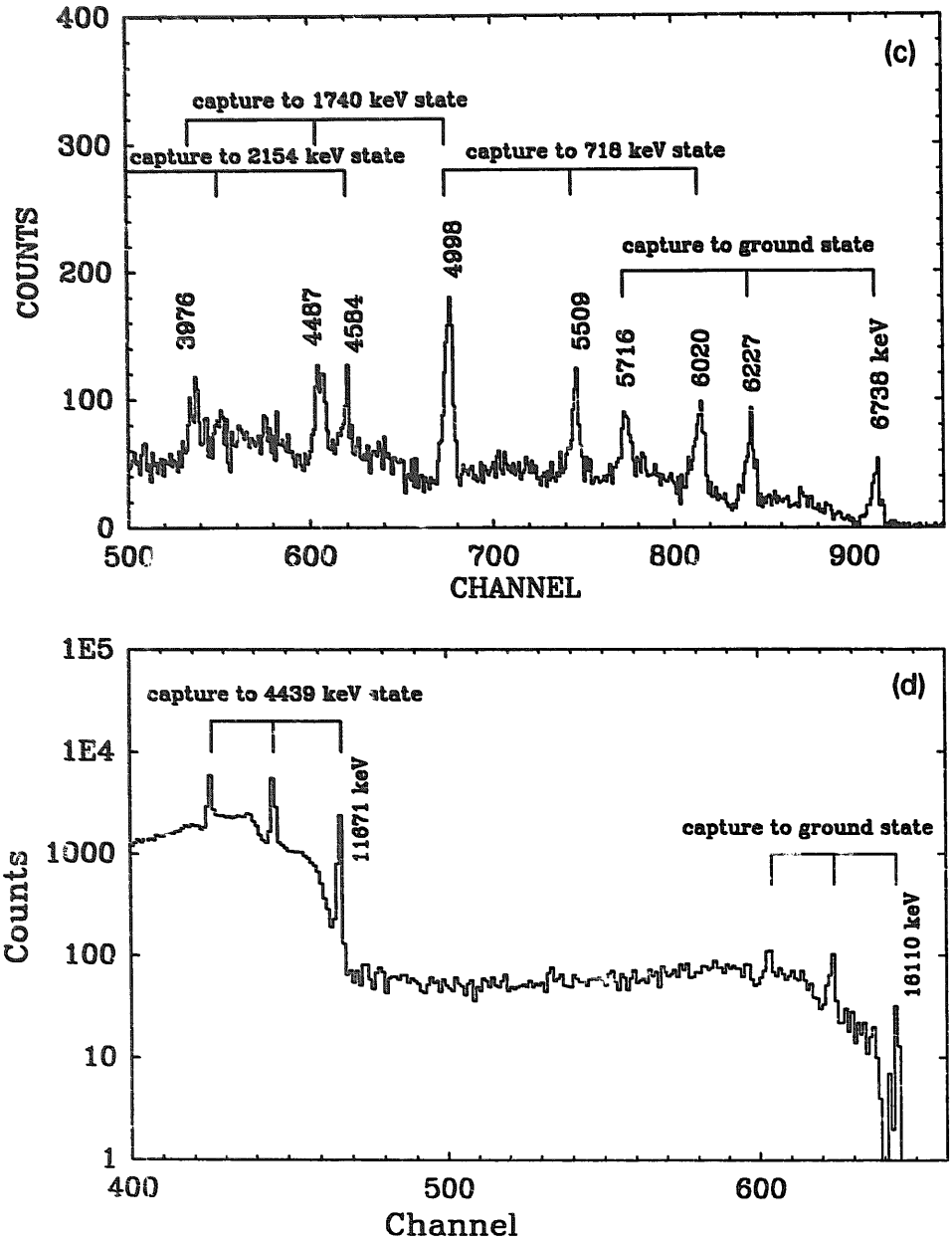

Fig. 5—continued.

S-factors provided by eq. (5). These S-factors are also plotted in fig. 7. The quoted uncertainties in the S-factors represent the combined uncertainties due to detector efficiency, statistical uncertainties, and quoted errors in the S-factors for the particle branches [4-7]). The S-factors are obviously plotted in fig. 7 at energies outside the range over which the branching ratio measurements were made (as indicated in fig. 6). The accuracy of this extrapolation is indicated in table 3 where the various S-factors and their respective uncertainties are evaluated at zero energy.

As noted above, angular distributions for the individual γ-rays were needed to infer the γ-ray S-factors from the yield ratios. These were measured at angles from

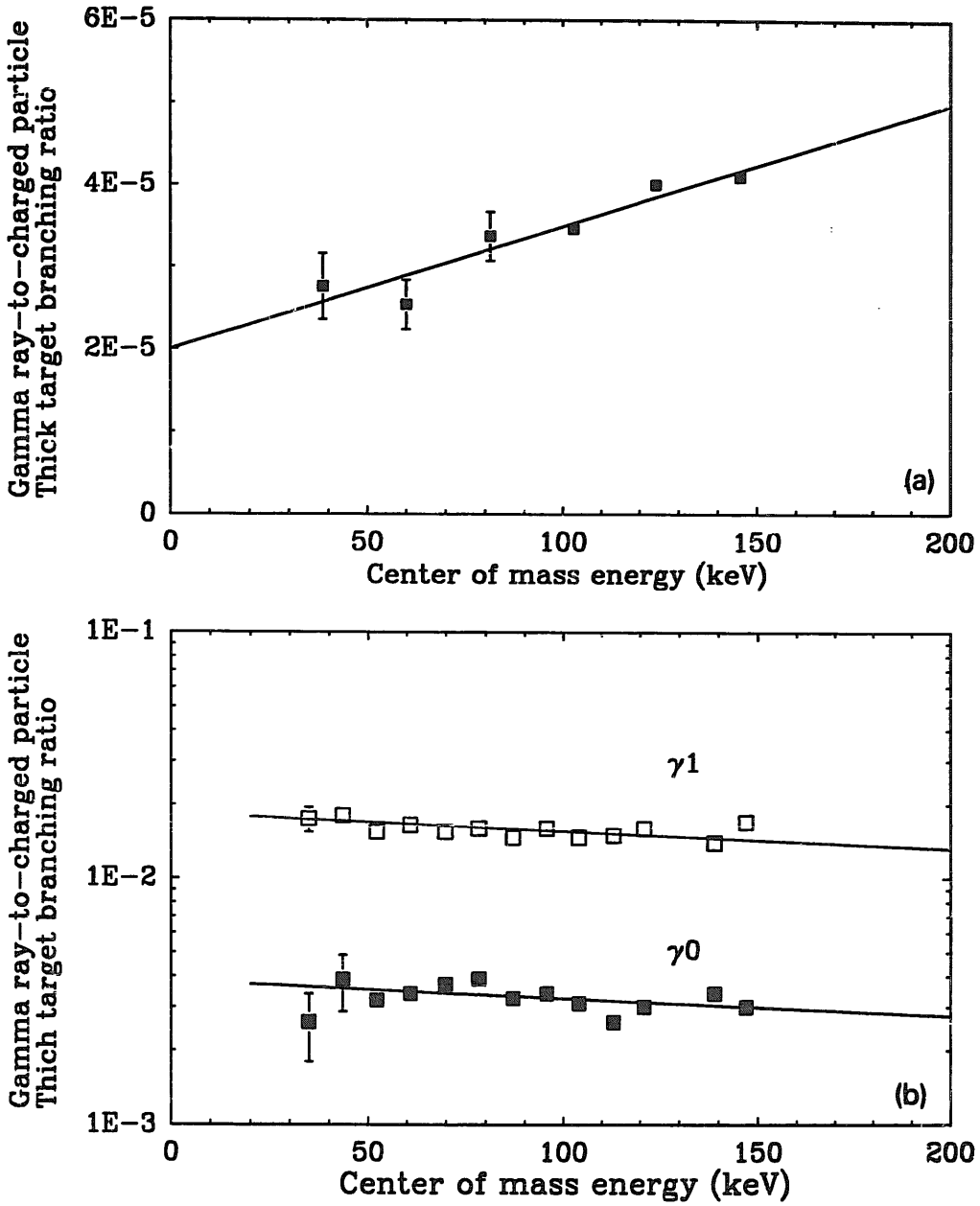

Fig. 6. Thick-target γ-ray-to-charged-particle branching ratios. Plotted in these figures is the quantity BR($E_{c.m.}$) as defined in eq. (2) in the text. (a)-(d) correspond respectively to the ^{6}Li, ^{7}Li, ^{9}Be and ^{11}B targets. The solid lines are the thick-target branching ratios as determined from eq. (4) in the text assuming the deduced S-factor.

0° to 150° to the forward beam direction and all are consistent at the 10% level with spatial isotropy with the exception of the transitions to the ground and excited states of ^{12}C at the 163 keV resonance. The angular distributions of the γ-rays emitted in the radiative capture to ^{12}C are given in fig. 8. Although the angular distributions presented in fig. 8 are derived from thick-target yields, the yields of these γ-rays at energies below the resonance are sufficiently small so as not to affect the angular distributions at the resonance by more than 2%. Small corrections ($\leq$10%) to the

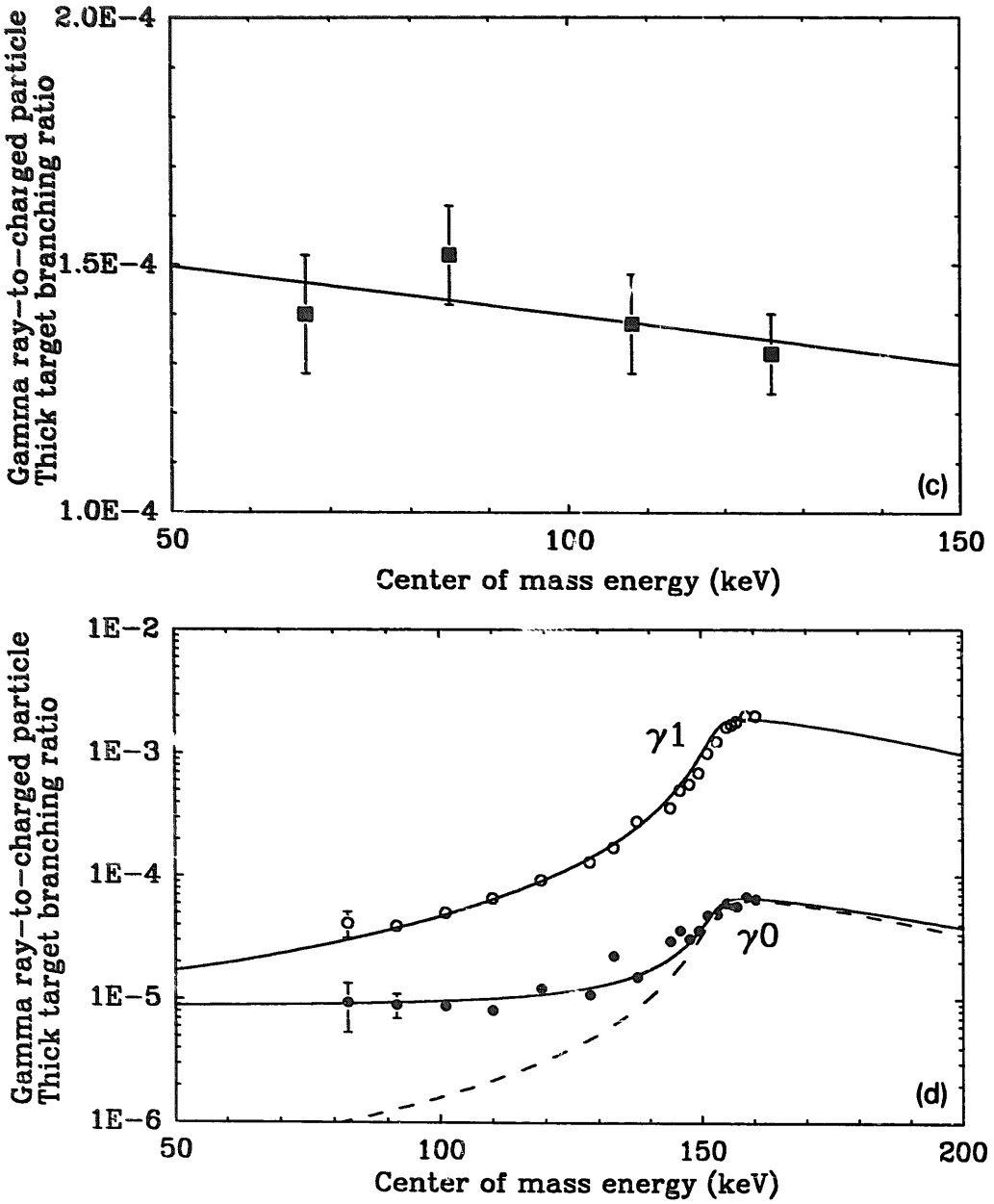

Fig. 6—continued.

S-factors for the capture reactions to the ground and first excited states in ^{12}C deduced using eqs. (4) or (5) were needed since these equations assumed isotropic γ-ray production. As indicated in fig. 8a, the distributions of the 4.44 and 11.67 MeV γ-rays agree with earlier measurements [15]) of these distributions at forward angles but are lower than the those of ref. [15]) at backward angles by about 10%. These fits could be improved if we assume relative angular distributions of:

$$1+0.05\cos(\Theta)+0.11\cos^2(\Theta),$$

$$1+0.10\cos(\Theta)+0.20\cos^2(\Theta),$$

TABLE 2

Gamma ray relative branching ratios and astrophysical S-factors for the radiative capture reactions studied in the present work. The energy dependences in the S-factors correspond to the center-of-mass energies of the proton-target system measured in MeV

Reaction	Final state	Branching ratio	S-factor (MeV · b)	$\Delta S/S$ [b]
$p+^{6}Li$	^{7}Be (0.0)	0.60	$3.9\times10^{-5}+2.4\times10^{-4}E$	0.15
	^{7}Be (0.429)	0.40	$2.6\times10^{-5}+1.6\times10^{-4}E$	0.15
$p+^{7}Li$	^{8}Be (0.0)	0.17	2.5×10^{-4}	0.15
	^{8}Be (3.04)	0.83	1.2×10^{-3}	0.15
$p+^{9}Be$	^{10}B (0.0)	0.22	9.2×10^{-4}	0.25
	^{10}B (0.718)	0.33	1.42×10^{-3}	0.25
	^{10}B (1.740)	0.33	1.42×10^{-3}	0.25
	^{10}B (2.154)	0.11	4.7×10^{-4}	0.25
$p+^{11}B$	^{12}C (0.0)	0.61 [a]	$2\times10^{-3}+10^{-6}/[(E-0.15)^2+7.3\times10^{-6}]$	0.20
	^{12}C (4.439)	0.39 [a]	$3\times10^{-5}/[(E-0.15)^2+7.3\times10^{-6}]$	0.15

[a]) The branching ratios to the ground and first excited states of ^{12}C are energy dependent. The values quoted for these transitions correspond to zero energy incident protons.

[b]) The relative S-factor uncertainty at a center-of-mass energy of 100 keV.

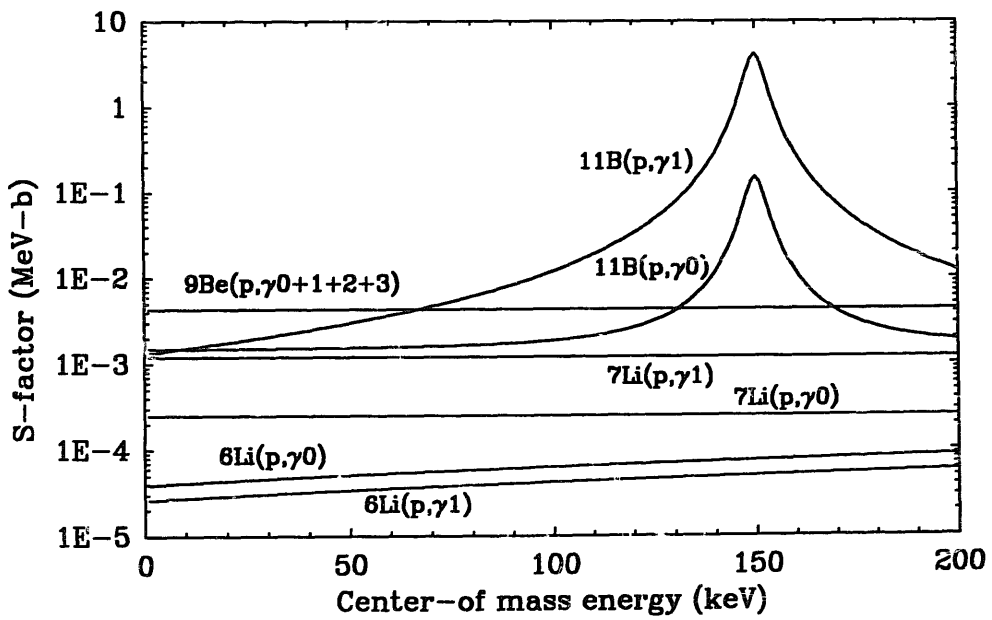

Fig. 7. Astrophysical S-factors for the radiative capture of protons on ^{6}Li, ^{7}Li, ^{9}Be and ^{11}B as determined from the branching-ratio measurements. In the case of ^{9}Be, we plot the combined S-factor for the transitions to the ground and first three excited states of ^{10}B.

TABLE 3

Experimentally determined astrophysical S-factors extrapolated to zero energy

Reaction	Final state (MeV)	S-factor (MeV · b)
$p+^6Li$	$^7Be(0.0)$	$(3.9\pm0.8)\times10^{-5}$
	$^7Be(0.429)$	$(2.6\pm0.6)\times10^{-5}$
$p+^7Li$	$^8Be(0.0)$	$(2.5\pm0.5)\times10^{-4}$
	$^8Be(3.04)$	$(1.2\pm0.2)\times10^{-3}$
$p+^9Be$	$^{10}B(0.0)$	$(9.2\pm2.5)\times10^{-4}$
	$^{10}B(0.718)$	$(1.4=0.4)\times10^{-3}$
	$^{10}B(1.740)$	$(1.4\pm0.4)\times10^{-3}$
	$^{10}B(2.154)$	$(4.7\pm1.5)\times10^{-4}$
$p+^{11}B$	$^{12}C(0.0)$	$(2.0\pm0.4)\times10^{-3}$
	$^{12}C(4.439)$	$(1.3\pm0.3)\times10^{-3}$

for the 4.44 and 11.67 MeV γ-rays, respectively. On the other hand, as indicated in fig. 8b, the distribution of the 16.11 MeV γ-ray appears markedly different than earlier measurements [15-16]) and is more in line with a quoted theoretical prediction [15]). The angular distribution of the 6.48 MeV γ-ray appears to be isotropic at the 15% level. The measured isotropy of the γ-radiation from the $^7Li(p, \gamma)^8Be$ reaction confirms the low-energy behavior noted by Mainsbridge [17]). There have been no reported angular distributions at low energies for the γ-rays emitted in the capture of protons by ^6Li or ^9Be nor of the 6.48 MeV γ-ray emitted in the decay of the 16.11 MeV level in ^{12}C to the 9.63 MeV level.

4. Calculations and comparisons

As noted in the introduction to this work, there are few data on proton radiative capture reactions on ^6Li, ^7Li, ^9Be, and ^{11}B at low energies with which to compare our present results. The reaction $^{11}B(p, \gamma)^{12}C$ has been well studied in the region of the resonance at $E_p = 163$ keV and the accepted value [8]) of the ground-state resonant-capture cross section of 5.5 μb agrees with the cross section we calculate from our derived S-factors and which is plotted in fig. 9.

To provide a theoretical reference point we compare our measurements to a simple direct-capture model. Our calculations almost identical that of Rolfs [18]). (For completeness, we present our definitions and conventions.) The reader is referred to Tombrello [19]) for a more general model. We employ a distorted-wave Born approximation with unit spectroscopic factor, use the long-wavelength limit and truncate at s-waves for the incoming channel. More realistic calculations including spin-dependent forces, structure amplitudes, and coupling to the break-up channels will be presented elsewhere. In the following the subscript p refers to the projectile proton and subscript T refers to the (inert) target nucleus. In this model the

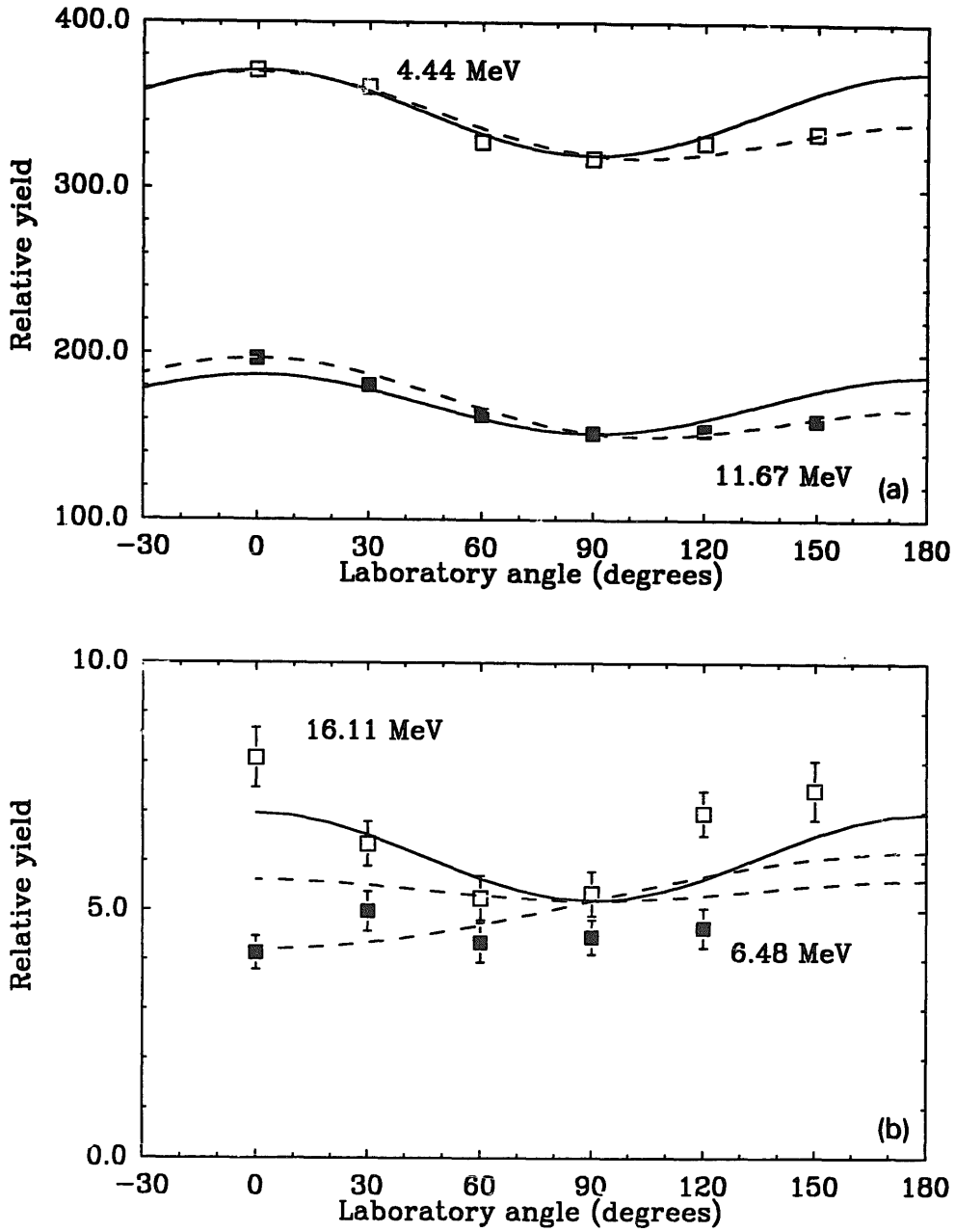

Fig. 8. Angular distributions of γ-rays from the reaction $^{11}B(p, \gamma)^{12}C$ at a bombarding energy of 165 keV. The upper and lower curves in (a) refer to the 4.44 and 11.67 MeV γ-rays. The dashed lines are our best fits to the data while the solid lines are the fits of Grant *et al.* [15]). The upper and lower sets of data in (b) refer to the angular distributions of the 16.11 and 6.48 MeV γ-rays. The dashed curves in (b) are previous measurements of the angular distribution of the 16.11 MeV γ-ray [15,16]) while the solid curve is the theoretical distribution given in ref. [15]).

differential cross section for direct photo-capture of a proton in the center-of-mass frame is given by

$$d\sigma = \frac{2\pi}{\hbar v_{rel}} \delta(E_p - E'_p - E_\gamma) \frac{d^3k_\gamma}{(2\pi)^3} |\langle f|H_{int}|i\rangle|^2 ,$$

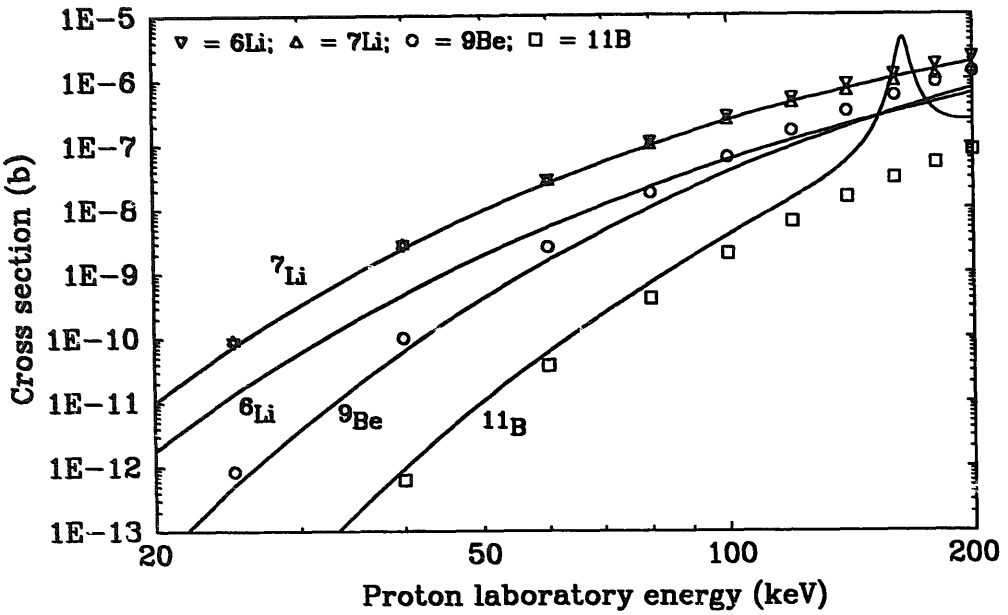

Fig. 9. Comparison of direct capture calculations (symbols) of the total cross sections for the ground-state transitions and cross sections evaluated (solid lines) using eq. (3) and the S-factors plotted in fig. 8 and listed in table 2. In the case of ^{9}Be, the 11% ground-state γ-ray branch given in table 2 was used to scale the total gamma-ray S-factor given in fig. 8.

where k_γ is the wave number of the outgoing gamma and $v_{\rm rel}$ is the relative velocity. Using the long-wavelength approximation, one has the matrix element:

$$\langle \mathrm{f}|H_{\rm int}|\mathrm{i}\rangle \simeq ie\mu d\sqrt{2\pi E_\gamma}\langle \mathrm{f}|\hat{\boldsymbol{\varepsilon}}\cdot\boldsymbol{r}|\mathrm{i}\rangle\,,$$

where $\mu = m_{\rm p}M_{\rm T}/(m_{\rm p}+M_{\rm T})$ is the reduced mass, and the center-of-mass dipole correction factor d is given by $d=(1/m_{\rm p}-Z_{\rm T}/M_{\rm T})$. Summing over final states, averaging over initial configurations, and integrating over angles, one finds:

$$\sigma(\mathrm{E1}) = \frac{16\pi\alpha}{9\hbar^4c^2}\,\frac{E_\gamma^3 d^2\mu^3}{k_{\rm c.m.}^3}\,\frac{(2J_{\rm f}+1)}{(2J_{\rm T}+1)}|\langle j'_{\rm p}\tfrac{1}{2}\,\tfrac{1}{2}-\tfrac{1}{2}|10\rangle|^2 R(\mathrm{E1})^2\,,$$

where $k_{\rm c.m.}$ is the incident center-of-mass wave number, $j'_{\rm p}$ is the final angular momentum of the bound proton, and the radial integral is given by

$$R(\mathrm{E1}) = \int_0^\infty \mathrm{d}r\, U_{\rm f}(r) r U_{\rm i}(r)\,.$$

In the above expression the initial and final wavefunctions have the standard form (with $l_{\rm i}=0$):

$$\Psi_{\rm i} = \sum_{m_{\rm p},M_{\rm i}} \langle J_{\rm T}M_{\rm T}j_{\rm p}m_{\rm p}|J_{\rm i}M_{\rm i}\rangle|J_{\rm T}M_{\rm T}\rangle|l_{\rm i}\tfrac{1}{2};j_{\rm p}m_{\rm p}\rangle\,,$$

$$|l_{\rm i}\tfrac{1}{2};j_{\rm p}m_{\rm p}\rangle = \frac{\sqrt{4\pi}}{k_{\rm c.m.}}\,\frac{U_{\rm i}(r)}{r}\,\mathcal{Y}_{[l_{\rm i}\frac{1}{2}]j_{\rm p}m_{\rm p}}(\hat{r},\chi)\,,$$

$$\Psi_f = \sum_{m'_p, M'_T} \langle J_T M'_T j_p m'_p | J_f M_f \rangle | J_T M'_T \rangle | l_f \tfrac{1}{2}; j'_p m'_p \rangle ,$$

$$| l_f \tfrac{1}{2}; j'_p m'_p \rangle = \frac{U_{l_f}(r)}{r} \mathcal{Y}_{[l_f \frac{1}{2}] j'_p m'_p}(\hat{r}, \chi) ,$$

where $\mathcal{Y}_{[ls]jm}(\hat{r}, \chi)$ is the standard coupled spin-angle function.

The radial wave functions including Coulomb and nuclear distortions are solved numerically using a second-order Numerov algorithm. The final bound-state radial wavefunction is normalized to unity while the initial radial wavefunction is calculated out to a maximum radius of 40 fm where it is matched onto the regular and irregular Coulomb functions and normalized to unit flux (so U_i is dimensionless). For the nuclear potential we use a central-only potential of Woods–Saxon form with diffusivity of 0.65 fm, half-density radius given by $R = r_0 A^{1/3}$ ($r_0 = 1.25$ fm), and depth adjusted to give the correct γ-energy.

Our calculations of the cross sections for capture of protons to the ground states of ^{7}Be, ^{8}Be, ^{10}B, and ^{12}C by ^{6}Li, ^{7}Li, ^{9}Be, and ^{11}B, respectively, are shown in fig. 9. These calculated cross sections may be compared to the cross sections derived from our measured ground-state S-factors, indicated in fig. 6 and tabulated in table 2. The cross sections derived from these S-factors, using eq. (3) are also plotted in fig. 9. Our calculations assume only a direct-capture reaction mechanism and hence the 163 keV resonance in the ^{11}B(p, γ)^{12}C reaction is not included in the calculations. Aside from this understood deviation, note the good agreement between the measured and calculated cross sections for the ^{7}Li, ^{9}Be, and ^{11}B reactions, particularly at the lowest measured energies. The measured cross section for the reaction ^{6}Li(p, γ)^{7}Be is, however, smaller than the calculated cross section over the entire range of the data by about a factor of five. Our direct-capture calculations for the reaction ^{6}Li(p, γ)^{7}Be likewise exceed the more realistic calculations of Barker [20]), in which a significant reduction of the matrix element results from initial-state interactions, in the energy range 40 to 200 keV by about a factor of three.

Our measured S-factors may likewise be used to generate thermonuclear reactivities [21]). By adding the contributions from the capture to the ground and excited states, we are able to generate total capture reactivities. The temperature range corresponding to the range of energies at which the branching ratio measurements were made is determined by the energy of the Gamow peak [21]). The temperature at which the Gamow peaks for the four reactions corresponds to the maximum energies at which the reactions were observed, i.e. about 170 keV, varies from 5.9×10^8 K for ^{6}Li to 3.4×10^8 K for ^{11}B. The reactivities calculated at temperatures up 5.0×10^8 K from the S-factors given in fig. 6 and table 2 are indicated in fig. 10a and may be compared to the tabulated reactivities of Caughlan and Fowler [22]) which are plotted in fig. 10b. There is good agreement between the reactivity derived for the reaction ^{6}Li(p, γ)^{7}Be from our measured S-factors and the reactivity for this reaction given by Caughlan and Fowler. There is likewise reasonable agreement for the reaction

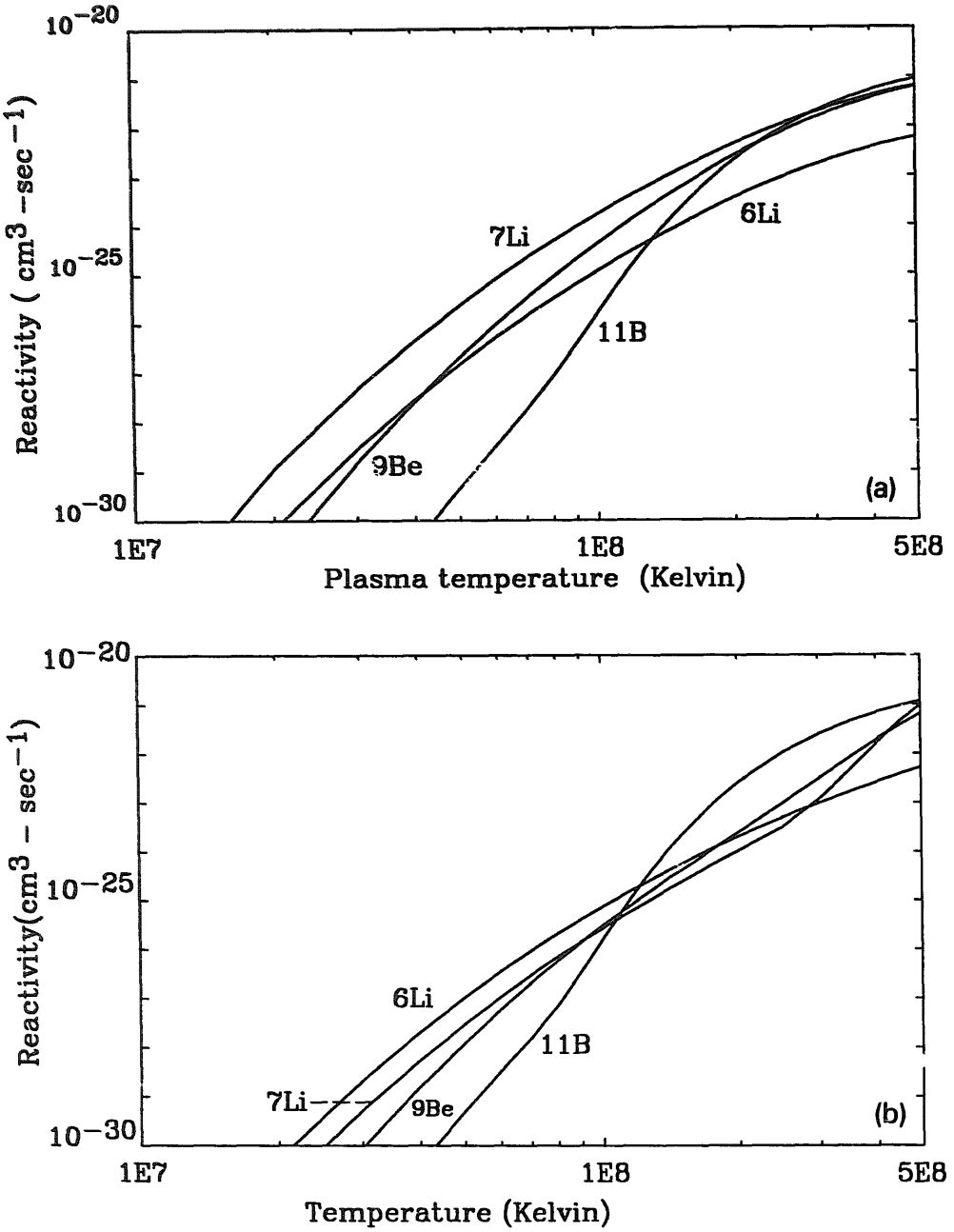

Fig. 10. (a) Total γ-ray thermonuclear reactivities calculated from the combined S-factors in fig. 8. (b) Plot of tabulated reactivities from Caughlan and Fowler [22]).

^{11}B(p, γ)^{12}C. In the case of the reaction ^{9}Be(p, γ)^{10}B, our reactivities exceed those of Caughlan and Fowler by about one order of magnitude at low temperatures and tend more closely toward rough agreement at higher temperatures. In the case of the reaction ^{7}Li(p, γ)^{8}Be, our reactivity exceeds that of Caughlan and Fowler by nearly two orders of magnitude except at the highest temperatures where the reactivity is dominated by the resonance in the reaction ^{7}Li(p, γ)^{8}Be at a proton bombarding energy of 441 keV [ref. [23])]. The discrepancy at low temperatures is

therefore a consequence of the fact that Caughlan and Fowler neglected any direct contribution to this reaction at low energies [24]). The source of the difference in the case of the reaction ^{9}Be(p, γ)^{10}B is, however, not clear.

5. Applications and conclusions

There are many areas of basic and applied science to which the present set of measurements may be applied. In this section we will discuss some of these areas very briefly. Details of these applications will be presented in forthcoming publications.

As noted in the introductory section of this report, one area to which radiative capture reactions on light nuclei may be applied is that of prompt γ-ray diagnostics of high temperature fusion plasmas. Our earlier BR(E) measurement of the γ-ray-to-charged-particle branching ratio of the D-^{3}He reaction has been the basis of γ-ray diagnostics systems on TFTR [25]) and JET [26]). Some of the present set of measurements were suggested a few years ago as the basis for similar diagnostics of the advanced fuel fusion plasmas [27]). The present results constitutes the data base for these diagnostics within the range of temperatures discussed in the preceding section and to within the uncertainties in the S-factors indicated in table 2. More detailed calculations of reactivities and reasonable count-rate calculations have been published [28]).

A second area of application of our present measurements is that of astrophysical nucleosynthesis. Current models of stellar evolution predict negligible quantities of ^{6}Li, ^{9}Be, and ^{11}B in the hydrogen burning phases of a star's development [21]). Primordial, or "Big Bang" nucleosynthesis might have been more generous in its production of these elements. Schramm and Wagoner [29]), for example, estimate the production of low levels of ^{6}Li and ^{11}B which survive the nucleosynthetic phase of an homogeneous Big Bang. Our measurement of the proton capture cross section by these isotopes, again at temperatures up to about 5×10^{8} K, will permit the production of ^{7}Be and ^{12}C by proton capture reaction to be evaluated. More recently, Boyd *et al.* [30]) have discussed the production of ^{9}Be in an inhomogeneous Big Bang model. Our measurement of the reaction ^{9}Be(p, γ)^{10}B should permit an estimate of the amount of ^{10}B produced. Together with the recent study [31]) of the reaction ^{10}B(p, γ)^{11}C, our results provide improved input data for calculations of the production of B and C in an inhomogeneous Big Bang.

A third area impacted by our present results is that of proton-induced γ-emission (PIGE), the nuclear γ-ray analogue of proton-induced X-ray emission (PIXE). The importance of these analytical tools is well described in numerous international biennial conferences [32]). We would only point out that our present results provide the data base for low energy and hence near surface PIGE analysis of Li, Be, and B. We would also caution that the relatively small cross sections for these reactions at low energies will limit the sensitivity of this analytical technique. We expect to

quantify the PIGE analysis of these elements using the proton capture reactions described in this report in the near future.

In conclusion we would emphasize that the results of this study close an important chapter in the field of nuclear physics. Together with earlier studies of proton capture reactions on the other light nuclei at low energies, the cross sections for all stable light nuclei through C have now been measured at energies sufficiently low so as to allow extrapolation to zero energy with the possible exception of ^{10}B for which an extrapolation to very low energies is complicated by the inferred [31]) resonance at $E_p = 10$ keV.

We would like to thank Claus Rolfs for a very helpful communication regarding our calculated cross sections. This work has been supported in part by USDOE Grants DE-FG02-87ER40342 and 88ER53276.

References

1) F.E. Cecil and F.J. Wilkinson, Phys. Rev. Lett. **53** (1984) 767
2) F.J. Wilkinson and F.E. Cecil, Phys. Rev. **C32** (1985) 2036
3) F.E. Cecil, D.M. Cole, R. Philbin, N. Jarmie and R. Brown, Phys. Rev. **C32** (1985) 690
4) A.J. Elwyn *et al.*, Phys. Rev. **C20** (1979) 1984
5) C. Rolfs and R.W. Kavanagh, Nucl. Phys. **A415** (1986) 179
6) A.J. Sierk and T. Tombrello, Nucl. Phys. **A210** (1973) 341
7) H.W. Becker, C. Rolfs and H.P. Trautvetter, Z. Phys. **A327** (1987) 341
8) F. Ajzenberg-Selove, Nucl. Phys. **A433** (1985) 1
9) F.E. Cecil *et al.*, Nucl. Instr. Meth. **B40/41** (1989) 934
10) C.A. Barnes *et al.*, Phys. Lett. **B197** (1987) 315
11) F.E. Cecil, F.J. Wilkinson, R. Ristenin and R. Rieppo, Nucl. Instr. Meth. **A234** (1985) 479
12) E. Waibel and B. Grosswendt, Nucl. Instr. Meth. **131** (1975) 133
13) D.L. Kennedy *et al.*, Nucl. Instr. Meth. **140** (1977) 519
14) J.F. Ziegler, (1989) unpublished
15) P.J. Grant *et al.*, Proc. Phys. Soc. (London) **A67** (1954) 751
16) D.S. Craig *et al.*, Phys. Rev. **103** (1956) 1414
17) B. Mainsbridge, Nucl. Phys. **21** (1960) 1
18) C. Rolfs, Nucl. Phys. **A217** (1973) 29
19) T. Tombrello and P. Parker, Phys. Rev. **131** (1963) 2582
20) F.C. Barker, Aust. J. Phys. **33** (1980) 159
21) D.D. Clayton, Principles of stellar evolution and nucleosynthesis (Univ. of Chicago Press, 1983)
22) G.R. Caughlan and W.A. Fowler, At. Data Nucl. Data Tables **40** (1988) 283
23) F. Ajzenberg-Selove, Nucl. Phys. **A490** (1988) 1
24) G.A. Caughlan, private communication (1989)
25) F.E. Cecil and S.S. Medley, Nucl. Instr. Meth. **A271** (1988) 628
26) D.A. Boyd *et al.*, Nucl. Fusion **29** (1989) 593
27) S.S. Medley, F.E. Cecil, D. Cole, M.A. Conway and F.J. Wilkinson, Rev. Sci. Instr. **56** (1985) 975
28) F.E. Cecil, H. Liu, J.C. Scorby and S.S. Medley, in Proc. Eighth Topical Conf. on high temperature plasma diagnostics, Reviews of Scientific Instruments, **61** (1990) 3223
29) D.N. Schramm and R. Wagoner, Ann. Rev. Nucl. Sci. **27** (1977) 37
30) R.N. Boyd and T. Kajino, Ap. J. **336** (1989) 155
31) M. Wiescher *et al.*, Phys. Rev. **C28** (1983) 1431
32) Proc. 5th Int. Conf. on PIXE and its Analytical Applications (Amsterdam) ed. Ronald D. Vis, Nucl. Instr. Meth. **B49** (1990)